Chinese Journal of
POLYMER SCIENCE

RESEARCH ARTICLE

https://doi.org/10.1007/s10118-026-3581-1
Chinese J. Polym. Sci.

Iron-based Catalysts Catalyzing Isoprene Polymerization: The Effect of Conjugated Groups in Cyanide-containing Electron Donors

Yao Liu[a,b,c], Yao-Guang Liu[d], Jun-Xin Xu[d], Qi Yang[a,b,c], Wen-Peng Zhao[a,b,c], Liang Fang[a,b,c*], Xiu-Juan Wang[a,b,c*], Heng Liu[a,b,c], Chun-Yu Zhang[a,b,c*], and Xue-Quan Zhang[a,b,c]

[a] *Key Laboratory of Advanced Rubber Material, Ministry of Education, School of Polymer Science and Engineering, Qingdao University of Science & Technology, Qingdao 266042, China*
[b] *Shandong Provincial College Laboratory of Rubber Material and Engineering, School of Polymer Science and Engineering, Qingdao University of Science & Technology, Qingdao 266042, China*
[c] *Key Lab of Rubber-Plastics, Ministry of Education/Shandong Provincial Key Lab of Rubber-plastics, School of Polymer Science and Engineering, Qingdao University of Science & Technology, Qingdao 266042, China*
[d] *Suzhou Uropod Precision Instruments Technologies Co., Ltd., Suzhou 215137, China*

Electronic Supplementary Information

Abstract In this study, the coordination pathways and decomposition behavior of azo-containing dicyano compounds within $Fe(acac)_3/Al^iBu_3$/donor ternary catalyst systems were systematically investigated *via in situ* Raman spectroscopy. Additionally, the modulating effect of conjugated moieties on the coordination interaction between cyanide groups and Fe ions was examined in detail. Experimental results demonstrate that isoprene polymerization catalyzed by azodicyanide mediated Fe-based catalytic systems proceeds *via* a coordination polymerization mechanism. Notably, the azo group does not directly participate in the coordination process; instead, it exerts a regulatory influence on the coordination capacity of the cyano group. Although thermal decomposition of the azo group occurs at elevated temperatures, it fails to initiate free radical polymerization of the isoprene monomer. Conjugated moieties including azo, vinyl, and benzene rings exert distinct impacts on the cyanide group. As electron-donating species, their Raman spectral characteristics reflect varying influences on cyanide coordination behavior. Density functional theory (DFT) calculations demonstrate that AIBN with azo groups as the conjugated moiety exhibits the most negative Gibbs free energy ($\Delta G°$=−222.71 kcal·mol^{-1}) for the coordination reaction with Fe^{2+}, indicating that the cyano groups in the azo-containing compound possess the strongest coordination capability with Fe^{2+}. The coordination effects of conjugated groups on the cyanide center follow the sequence: azo > carbon-carbon double bond > benzene ring, where azo groups show the most significant coordination enhancement. These theoretical findings are consistent with the observed polymerization activity, suggesting that rational design of electron donors can be guided by theoretical calculations.

Keywords Iron-based catalysts; Polyisoprene; Azo group; Raman spectroscopy; Density functional theory (DFT)

Citation: Liu, Y.; Liu, Y. G.; Xu, J. X.; Yang, Q.; Zhao, W. P.; Fang, L.; Wang, X. J.; Liu, H.; Zhang, C. Y.; Zhang, X. Q. Iron-based catalysts catalyzing isoprene polymerization: the effect of conjugated groups in cyanide-containing electron donors. *Chinese J. Polym. Sci.* https://doi.org/10.1007/s10118-026-3581-1

INTRODUCTION

In the field of tire manufacturing, 3,4-polyisoprene rubber is expected to become the preferred material for producing high-performance tires owing to its excellent wet skid resistance and low rolling resistance.[1–7] With the development of transition metal-based coordination polymerization catalysts, most Ziegler-Natta catalyst systems, which are composed of transition metals (such as Ti, Co, Nd, and Fe) and organoaluminum compounds, can initiate the 3,4-selective polymerization of isoprene to obtain 3,4-polyisoprene rubber.[8–20] Among the various catalyst systems, iron-based catalysts are considered highly promising because of their abundant reserves, low cost, exceptional biocompatibility, ease of preparation, and stability under broad polymerization conditions.[21–28] In iron-based catalyst systems, electron-donating ligands, as key components, exert a significant regulatory effect on the catalytic activity and selectivity of catalysts.[29–32] In previous research, *N*-containing compounds (such as dithiooxamide, *N,N'*-dimethyl dithiooxamide, 2-cyanopyridine, and 2-hydroxybenzimidazole) have been used as electron donors to enhance the catalytic activity.[33–35] The $Fe(acac)_3/Al^iBu_3$/*N*-containing compound (such as bipyridine and 1,10-phenanthroline) catalytic system was selected for the polymerization of isoprene, and polyisoprene with moderate amounts of 1,4-structural units and 3,4-structural units was suc-

* Corresponding authors, E-mail: fangliang@qust.edu.cn (L.F.)
E-mail: wangxj@qust.edu.cn (X.J.W.)
E-mail: cyzhang@qust.edu.cn (C.Y.Z.)
Received December 22, 2025; Accepted January 20, 2026; Published online April 17, 2026

cessfully prepared.[36] Generally, most iron-based catalysts constructed with nitrogen-containing compounds are temperature sensitive and prone to deactivation under high-temperature conditions. This characteristic demonstrates the generally poor thermal stability of such catalysts.[37–39] The defects in low-temperature polymerization were finally solved by using AIBN as the electron-donating ligand to construct the Fe(2-EHA)$_3$/Al^{i}Bu$_3$/AIBN catalytic system for the coordination polymerization of isoprene. This catalytic system exhibited high catalytic activity and the resulting polymer had a high molecular weight without gel formation. The chain structure of polyisoprene is dominated by *cis*-1,4-units (46%–51%) and 3,4-units (40%–46%), whereas the content of 1,2-units is only 4%–9%.[40] Notably, the catalyst preparation method, type and amount of alkylaluminum, and polymerization temperature exert no significant influence on the microstructure of polyisoprene. A catalytic system constructed using the *N*-containing compound IITP (as an electron donor) and Fe(acac)$_3$/Al^{i}Bu$_3$ has been reported to be applicable for the synthesis of polyisoprene, polybutadiene, and their block copolymers.[25,26] This catalytic system exhibits high activity under high-temperature conditions, and the resulting polymers possess a relatively high molecular weight.[28] Recently, an iron-based catalyst incorporating AIBN as a third component catalyzed the copolymerization reactions of butadiene and isoprene. Even when the [Al]/[Fe] molar ratio was varied, the prepared copolymers maintained excellent structural stability, and no gel formation was observed.[27] Furthermore, the introduction of PPh$_3$ into the Fe(acac)$_3$/Al^{i}Bu$_3$/AIBN iron-based catalytic system for the polymerization of butadiene enables effective regulation of polymer crystallinity. This finding has rekindled research interest in diene polymerization systems using AIBN as an electron donor.[41]

However, the mechanism of isoprene polymerization catalyzed by the AIBN-containing iron-based catalytic system remains controversial. This is primarily because the AIBN molecule contains both azo and cyano moieties, which have the potential to coordinate with the metal center. Additionally, the azo group is prone to thermal decomposition, which may lead to the formation of a free-radical reaction pathway in the system, thereby interfering with the determination of the dominant polymerization mechanism. However, free-radical polymerization alone cannot efficiently achieve isoprene polymerization. For instance, an atom transfer radical polymerization (ATRP) system based on Fe/AIBN/PPh$_3$ can realize living/controlled polymerization of styrene and methyl methacrylate monomers at high temperatures, but it is not applicable to conjugated diene monomers such as isoprene.[42–48]

In addition, the paramagnetism of iron ions renders nuclear magnetic resonance (NMR) spectroscopy unable to monitor the dynamic changes in the catalytic system, which poses a challenge to the characterization of coordination structures. In infrared (IR) spectroscopy, the characteristic absorption peak of the azo group (1620–1570 cm^{-1}) exhibits a weak intensity and is prone to overlap with other peaks, making accurate tracking difficult and further complicating the detection process.[49,50] In recent years, *in situ* variable-temperature Raman spectroscopy, as a versatile analytical technique, has captured subtle frequency changes. Although the characteristic peaks of the azo groups exhibit weak signals in solvents and are prone to overlap, the Raman peak of the C—C—N stretching mode of N≡C—C—N=N can still be traced, providing an effective approach for the characterization of coordination structures. Furthermore, the continuous advancement of molecular simulation calculation techniques has enabled the elucidation of the electronic properties and thermodynamic trends of catalytic systems at the atomic level. Such computational tools can also perform quantitative analyses of the electrostatic interactions, charge redistribution, and energy feasibility during the coordination process.[51–53] Density functional theory (DFT) theoretical studies have proven to be a useful tool for nucleophilic, electrophilic, and cyclo-addition reactions, allowing not only the distinction between kinetic and thermodynamic effects but also their quantitative estimation.[54–56] The Gibbs free energy change (ΔG) of the coordination reaction was obtained *via* DFT calculations. The coordination ability between ligands and metal ions can be quantitatively compared by the value of ΔG: the more negative the ΔG value, the more stable the binding between the ligand and Fe^{2+} and the stronger the coordination ability. These calculation results provide key support for an in-depth understanding of the relevant complex chemical phenomena. The synergistic development of *in situ* variable-temperature Raman spectroscopy and DFT calculations not only enables the investigation of the polymerization mechanism of isoprene catalyzed by AIBN-containing iron-based catalysts but also offers theoretical guidance for the molecular design of electron-donating ligands.[57]

In this study, a strategy combining Raman spectroscopy measurements, theoretical calculations, and polymerization experiments was adopted to investigate the effect of the azo group on the coordination interaction between cyano groups and Fe^{2+} during the polymerization process. The specific research contents are as follows: (1) *in situ* variable-temperature Raman spectroscopy was used to detect the changes in the Raman peak of the C—C—N stretching mode to analyze the coordination behavior and decomposition characteristics of the azo group. The evolution of the characteristic absorption peaks during the coordination of the cyano group with Fe^{2+} was also investigated. Combined with the natural population analysis (NPA) charge changes before and after the coordination reaction obtained from DFT calculations, the coordination mechanism was explained. (2) Dicyano compounds with different conjugated groups were designed as electron-donating ligands for comparison. The electrostatic potential (ESP) distribution on the surface of the electron-donating ligands was calculated and a coordination model was constructed to calculate ΔG of the coordination reaction. By combining the polymerization activity data, the specific role of the azo group in the isoprene polymerization catalyzed by the system was clarified.

EXPERIMENTAL

Materials

Iron(III) acetylacetonate (Fe(acac)$_3$, 0.05 mol·L^{-1}), Iron(III) 2-ethylhexanoate (Fe(2-EHA)$_3$, 0.05 mol·L^{-1}), 2,2′-azobis(2-methylpropionitrile) (AIBN/D$_1$, 0.02 mol·L^{-1}), 2,2'-azodi(2-methylbutyronitrile) (AMBN, 0.02 mol·L^{-1}), 2,2'-azobis(2,4-dimethyl) valeronitrile

(ABVN, 0.02 mol·L^{-1}), dimethyl 2,2'-azobis(2-methylpropionate) (AIBME, 0.02 mol·L^{-1}), isobutyronitrile (IBN, 0.02 mol·L^{-1}), trimethylacetonitrileand (t-BuCN, 0.02 mol·L^{-1}) and 1,4-dicyano-2-butene (D_2, 0.02 mol·L^{-1}) were purchased from Sinopharm Chemical Reagent Co., Ltd. (Shanghai, China) and diluted with toluene to the appropriate concentration. 1,4-Phenylenediacetonitrile and 1,3-phenylenediacetonitrile were purchased from Sinopharm Chemical Reagent Co., Ltd. (Shanghai, China) and used in the synthesis experiments. Triisobutyl aluminum (Al^{i}Bu$_3$, TIBA) was purchased from Macklin and diluted to 1.0 mol·L^{-1} in toluene. Polymerization-grade isoprene (IP) was purchased from Fluka, refluxed over CaH_2 for 4 h, and distilled before use. Toluene, *N,N*-dimethylformamide (DMF), and dichloromethane (DCM) were refluxed over sodium/diphenylketone under nitrogen and distilled before use. All other commercial chemicals were used as received.

Design and Synthesis of Electron Donor

To investigate the effect of the presence of an azo group in the electronic donor on polymerization, the azo group was replaced with a benzene ring, and $\alpha^1,\alpha^1,\alpha^3,\alpha^3$-tetramethyl-1,3-benzenediacetonitrile (D_3) with meta-substitution on the benzene ring and $\alpha^1,\alpha^1,\alpha^4,\alpha^4$-tetramethyl-1,4-benzenediacetonitrile (D_4) with *para*-substitution on the benzene ring were designed and synthesized. Synthesis steps: into a 250 mL single neck flask was placed sodium hydride 60% (5.4 g, 134.5 mmol) in DMF (100 mL) at –15 °C. 1,3-Phenyldiacetonitrile (5 g, 32 mmol) was slowly added to the solution and the mixture was stirred for 0.5 h. The reaction mixture was treated with methyl iodide (8.4 mL, 134.5 mmol). The mixture was warmed to room temperature and stirred for 12 h. The reaction mixture was poured into ice water (600 mL) until the product was precipitated. The precipitate was filtered and washed with cold water to obtain the intermediate compound D_3, pink liquid, (5.2 g, yield 76%). In the synthesis step, the starting material 1,3-phenyldiacetonitrile (5 g, 32 mmol) was replaced with 1,4-phenyldiacetonitrile (5 g, 32 mmol), and the same steps were repeated to obtain D_4, which is a white solid (5.4 g, yield 79%). Data for D_3: ^{1}H-NMR (500 MHz, $CDCl_3$, δ, ppm): 7.56 (s, 1H, Ar-H), 7.44 (d, 3H, Ar-H), 1.75 (s, 12H, CH_3). ^{13}C-NMR (126 MHz, $CDCl_3$, δ, ppm): 142.10, 129.37, 124.47, 123.95, 121.46, 37.04, 28.87. FTIR (KBr, cm^{-1}): 3056 (w), 2984 (s), 2939 (s), 2232 (m), 1607 (m), 1489 (m), 1463 (m), 1425 (m), 1371 (m), 1224 (m), 1090 (m), 798 (s), 702 (s). HRMS (*m/z*): calculated for $C_{14}H_{16}N_2$: 213.1391, found 235.1213 [M+Na]$^+$. The NMR spectra of D_3 are shown in Figs. S1 and S2 (in the electronic supplementary information, ESI). Data for D_4: ^{1}H-NMR (400 MHz, $CDCl_3$, δ, ppm): 7.50 (s, 4H, Ar-H), 1.73 (s, 12H, CH_3). ^{13}C-NMR (101 MHz, $CDCl_3$, δ, ppm): 141.17, 126.04, 124.24, 77.53, 37.04, 28.86. FTIR (KBr, cm^{-1}): 3034 (w), 2991 (s), 2918 (m), 2238 (s), 1646 (m), 1546 (m), 1475 (m), 1417 (m), 1368 (m), 1255 (m), 1119 (m), 1017 (m), 834 (s). HRMS (*m/z*): calculated for $C_{14}H_{16}N_2$: 213.1391, found 213.1391. The NMR spectra of D_4 are shown in Figs. S3 and S4 (in ESI).[58]

Polymerization Procedure

All manipulations were performed under a dry nitrogen atmosphere. The detailed polymerization procedure is described as a typical example. A hexane solution of isoprene (1.8 mol·L^{-1}, 16.34 mL) was placed in an oxygen- and moisture-free ampoule capped with a rubber septum. Then, Fe(acac)$_3$, the electron donor and Al^{i}Bu$_3$ at the designed ratios were charged sequentially into the above ampoule. Polymerization was performed at 50 °C for 4 h and terminated by adding 2.0 mL of acidified ethanol containing the antioxidant reagent 2,6-di-tert-butyl-4-methylphenol (BHT, 1.0 wt%). A large amount of ethanol was added and washed repeatedly to convert the active end group into an inactive salt, which could be dissolved in ethanol or water. Finally, the obtained product was dried to a constant weight under a vacuum at 50 °C. The polymer yield was determined by gravimetric analysis.

Characterization

Gel permeation chromatography (GPC) utilizing an AGILENT Technologies high-temperature system, 1260 Infinity II, was employed to determine the number-average molecular weight (M_n) and polydispersity index (PDI) of the polymer samples at 150 °C, and a flow rate of 1.0 mL·min^{-1} with 1,2,4-trichlorobenzene as the solvent was used for this analysis. The NMR spectra of the samples were recorded on a BRUKER AVANCE NEO 400 MHz spectrometer using $CDCl_3$ and $C_6D_4Cl_2$ as solvents at ambient temperature and tetramethylsilane (TMS) as an internal standard. Differential scanning calorimetry (DSC) measurements were performed on a NETZSCH 204 F1 diamond instrument under nitrogen atmosphere at a heating rate of 10 °C·min^{-1}. Microstructure analysis of the electronic donors was conducted by Raman spectroscopy using a UPD-785M spectrophotometer. Microstructure analysis of the synthetic materials was conducted by Fourier transform infrared (FTIR) spectroscopy using a BRUKE VERTEX-70 spectrometer.

RESULTS AND DISCUSSION

Polymerization of Different Azo Compounds as Electron Donors

The role of the donor in the catalytic system can generally be summarized as follows: (a) stabilizing metal centers in a low-valence state by filling orbit vacancies, (b) preventing the deactivation of active species, and (c) facilitating selective coordination and insertion of the active species for 1,3-butadiene.[31,34] In this research, several compounds containing azo groups (AIBN, AIBME, ABVN, AMBN) were chosen as electron donors and combined with Fe(acac)$_3$/Al^{i}Bu$_3$ to create a ternary catalyst system. Subsequently, this catalytic system was employed to mediate the polymerization of isoprene to elucidate the distinct roles of the cyano and azo moieties within the AIBN molecular framework. The outcomes of the isoprene polymerization are shown in Table 1. Fig. 1 depicts the effects of varying the feed ratios of the electron donors, polymerization temperatures, and reaction durations on the polymerization process. Notably, when serving as electron donors for iron-based catalysts, AIBN, ABVN, and AMBN exhibit high efficiency in initiating polymerization under conditions of low monomer/catalyst molar ratio, achieving yields exceeding 96%. In contrast, AIBME, which contains an ester moiety, afforded relatively low yields (<17.76%). This may be attributed to the weaker coordination interaction between the ester group in the AIBME molecule and Fe compared to other cyano-containing compounds (AIBN, ABVN, and AMBN). Meanwhile, the ester group exhibits a larger steric hindrance effect, which hinders the coordination of monomers with the active centers, thereby reducing the polymerization activity and increasing the proportion of 3,4-units in the polymer. Among the

Table 1 Effect of catalyst component under various conditions on the polymerization behavior of IP, St and MMA. [a]

Run	Donor	[M/Fe] [b]	Temperature (°C)	Time (h)	Yield (%)	M_n [c] (×10^4)	PDI [c]	T_g [d] (°C)	Microstructure [e] (%)		
									3,4	1,2	1,4
1	AIBN	2000	50	4	99.60	16.0	1.98	−18.9	46.6	5.0	48.5
2		4000	50	4	98.75	21.1	1.86	−18.8	47.2	5.1	47.7
3		6000	50	4	99.06	26.8	1.76	−18.7	48.5	5.1	46.4
4		12000	50	1	82.31	25.3	1.99	−17.9	48.0	6.0	46.0
5		12000	70	1	91.78	35.2	1.86	−18.5	47.1	7.0	45.9
6	AIBME	2000	50	4	17.76	11.6	2.84	−15.9	50.8	4.4	44.8
7		4000	50	4	8.16	17.5	2.94	−17.3	51.8	4.5	43.7
8		6000	50	4	5.39	22.4	2.06	−14.5	50.8	5.6	43.6
9		12000	50	1	0	–	–	–	–	–	–
10		12000	70	1	0.33	–	–	–	–	–	–
11	ABVN	2000	50	4	98.93	23.3	2.15	−20.7	46.7	5.1	48.2
12		4000	50	4	97.89	28.6	2.09	−17.8	46.6	5.9	47.5
13		6000	50	4	97.09	31.6	2.11	−18.3	47.0	6.3	46.7
14		12000	50	1	15.53	28.6	1.86	−20.1	46.2	7.8	46.0
15		12000	70	1	84.39	33.3	1.95	−19.1	44.6	8.4	47.0
16	AMBN	2000	50	4	99.85	23.0	2.21	−19.3	47.1	5.3	47.6
17		4000	50	4	98.90	25.7	2.29	−17.0	48.6	5.0	46.4
18		6000	50	4	97.81	30.4	2.08	−18.9	48.5	5.8	45.7
19		12000	50	1	76.61	21.8	2.37	−19.6	45.9	7.2	46.9
20		12000	70	1	86.55	31.1	1.90	−18.1	43.5	6.1	50.4
21	IBN	2000	50	4	– [f]	–	–	–	–	–	–
22	*t*-BuCN	2000	50	4	–	–	–	–	–	–	–
23 [g]	AIBN	2000	50	4	–	–	–	–	–	–	–
24 [h]	AIBN	2000	50	4	–	–	–	–	–	–	–

[a] Polymerization conditions: [IP]=1.8 mol·L^{-1}, [Donor]/[Fe]=3, [Al]/[Fe]=20, in hexane; [b] M=monomer; [c] GPC data by trichlorobenzene versus polystyrene standards; [d] Measured using DSC; [e] Determined by NMR; [f] "–" not determined; [g] Monomer: St, [St]=2.0 mol·L^{-1}; [h] Monomer: MMA, [MMA]=2.0 mol·L^{-1}.

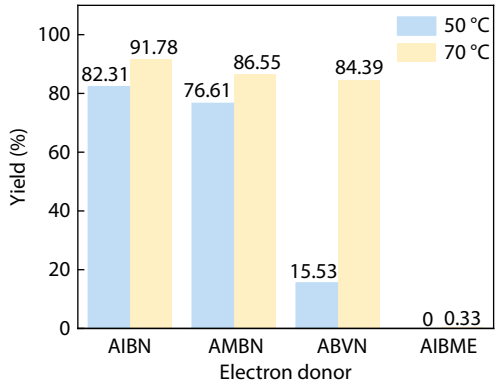

Fig. 1 Effect of electron donor on polymerization behaviors at different temperatures. Polymerization conditions: [IP]=1.8 mol·L^{-1}, [IP]/[Fe]=12000, [Donor]/[Fe]=3, [Al]/[Fe]=20, for 1 h, in hexane.

three electron donors (AIBN, ABVN, and AMBN), polymerization activity followed the order AIBN > AMBN > ABVN. In particular, within the AIBN system, high activity was retained, even at [IP]/[Fe]=12000. This suggests that the carbon chain length between the N=N double bond and cyano group in the electron donor modulates the polymerization activity. In other words, the azo group influences the electron cloud density of the cyano group, which subsequently affects the coordination ability of the Fe active center with the isoprene monomer. Furthermore, polymerization experiments using isobutyronitrile (IBN) and trimethylacetonitrile (*t*-BuCN) as electron-donating additives under identical conditions failed to initiate polymerization, indirectly highlighting the critical role of the azo group in cyano coordination.

Raman Testing of the ABVN/Fe(2-EHA)$_3$/Al^{i}Bu$_3$ Catalytic System

Owing to concentration and solvent limitations, the ABVN, Fe(2-EHA)$_3$ and Al^{i}Bu$_3$ systems, which exhibited higher solubility in n-hexane, were utilized for Raman testing. In the Raman spectra, a single intense peak in the region of 2285–2200 cm^{-1} is attributed to the C≡N stretching vibrational mode (Figs. 2–4). The Raman peak of the C≡N stretching mode for IBN is located at 2247 cm^{-1} and the Raman peak of the C≡N stretching mode for ABVN is located at 2243 cm^{-1} (Fig. 2). This is because the azo group in ABVN transmits a weak electron-donating inductive ef-

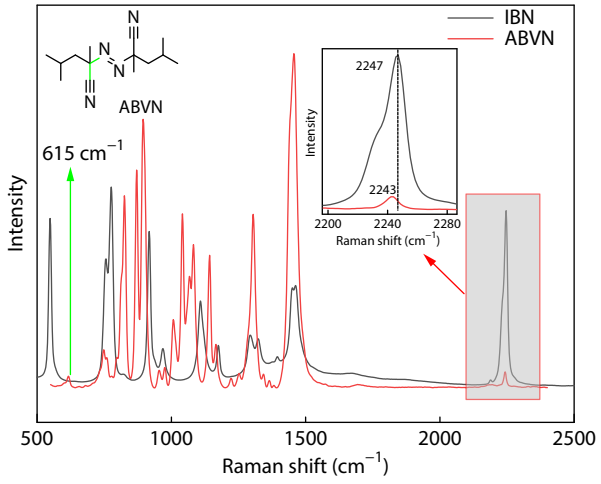

Fig. 2 Raman spectra of IBN and ABVN.

https://doi.org/10.1007/s10118-026-3581-1

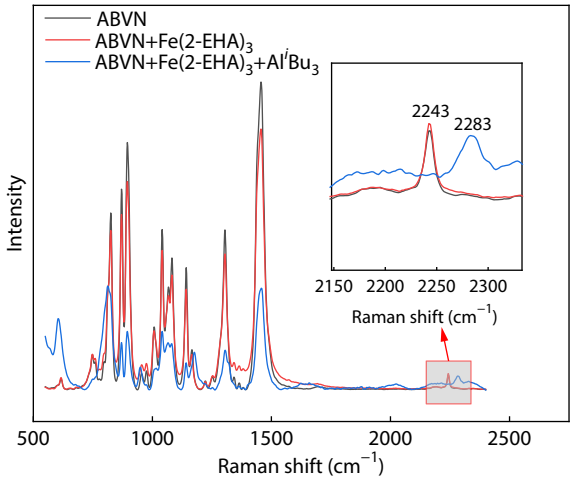

Fig. 3 Raman spectra of ABVN, ABVN/Fe(2-EHA)$_3$, and ABVN/Fe(2-EHA)$_3$/Al^{i}Bu$_3$.

fect through the σ bond, decreasing the electron cloud density of the nitrogen atom in the cyano group, slightly weakening the effective bond strength of the C≡N bond, and reducing the bond force constant, resulting in a red-shift of the C≡N stretching mode to 2243 cm^{-1}. The Raman peak at 615 cm^{-1} is located in the C—C—N stretching mode of the N≡C—C—N=N moiety in ABVN, and the Raman peak of the C≡N stretching mode for ABVN is located at 2243 cm^{-1}. Upon mixing ABVN with Fe(2-EHA)$_3$ ([ABVN]/[Fe]=3), no discernible changes were observed in the characteristic Raman spectrum peaks. Subsequently, the addition of Al^{i}Bu$_3$ resulted in a blue shift of the C≡N stretching mode for ABVN to 2283 cm^{-1} (Figs. 2–4). And as shown in Fig. S5 (in ESI), when only ABVN and Al^{i}Bu$_3$ were mixed (without other compounds), the Raman peak of the C≡N stretching mode for ABVN appeared at 2243 cm^{-1} with no discernible shift. This phenomenon arises from the reduction of Fe^{3+} to Fe^{2+} by alkylaluminum, accompanied by the dissociation of one 2-EHA ligand, which creates vacant coordination sites for the cyano group to bind to the iron center. The observed blue-shift of the C≡N stretching mode for ABVN after coordination with Fe^{2+} can be rationalized using natural population analysis (NPA) charge data (Table 2) and combined with related literature.[57] During coordination, the cyano nitrogen (N_{CN}) donates σ electrons to Fe^{2+}, causing its negative charge to decrease from $-0.304e^-$ (free ABVN) to $-0.251e^-$ (ABVN coordinated with Fe^{2+}), corresponding to a charge change (ΔQ) of $+0.053e^-$. The positive charge of the cyano carbon (C_{CN}) increased from $0.281e^-$ to $0.377e^-$ (ΔQ=$0.096e^-$). These changes result in an elevation of the C≡N charge separation ($\Delta\Delta Q$(C—N)) from $0.585e^-$ to $0.628e^-$. This caused an increase in the force constants ($k_{C\equiv N}$) in accordance with the increase in C≡N charge separation ($\Delta\Delta Q$(C—N)). According to the harmonic oscillation formula, a larger force constant directly raises the vibrational frequency, ultimately manifesting as a Raman blue-shift to 2283 cm^{-1}. In addition, the stability of the three systems was investigated using *in situ* variable-temperature Raman spectroscopy. As illustrated in Figs. S6 and S7 (in ESI), the Raman peak of the C—C—N stretching mode for ABVN and ABVN/Fe(2-EHA)$_3$ remained intact after heating at 50 °C for 4 h. However, upon heating at 70 °C for 4 h, the 615 cm^{-1} peak completely disappeared and the Raman peak of the C≡N stretching mode is red-shifted, indicating the complete decomposition of azo group. For the ABVN/Fe(2-EHA)$_3$/Al^{i}Bu$_3$ system, the Raman peak of the C≡N stretching mode was slightly and gradually red-shifted with increasing heating time at 50 °C. This phenomenon indicates decomposition of the azo group, leading to a change in the coordination ability between N_{CN} and Fe^{2+} ions. The force constants ($k_{C\equiv N}$) decreased, leading to a reduction in the vibration frequency. Consequently, the Raman peak of the C≡N stretching mode showed a red shift. These results indicated that free radicals were generated by the decomposition of ABVN at 50 °C. The Fe(acac)$_3$/Al^{i}Bu$_3$/AIBN iron-based catalytic system was employed for the polymerization of

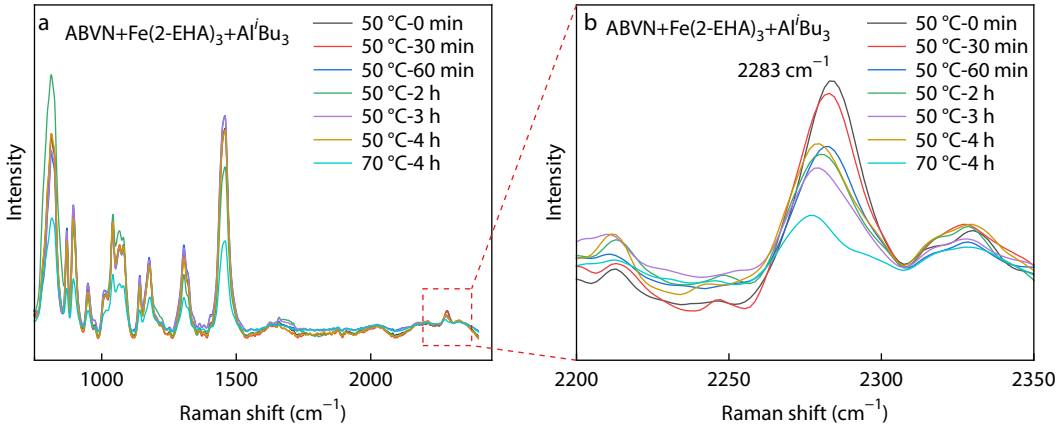

Fig. 4 Raman spectra of ABVN/Fe(2-EHA)$_3$/Al^{i}Bu$_3$ under varied heating conditions: (a) full view; (b) magnified view of the 2200–2350 cm^{-1} range region in (a).

Table 2 Calculated C_{CN} and N_{CN} NPA charges (e^-) (ΔQ) and C≡N charge separation ($\Delta\Delta Q$ (C—N)) in ABVN and ABVN-Fe^{2+}.

System	Q (C_{CN})	Q (N_{CN})	ΔQ (C_{CN})	ΔQ (N_{CN})	$\Delta\Delta Q$ (C—N)
ABVN	0.281	–0.304	–	–	0.585
ABVN-Fe^{2+}	0.377	–0.251	+0.096	+0.053	0.628

"–": reference state. $\Delta\Delta Q$ (C—N) = |Q (C_{CN}) – Q (N_{CN})|.

styrene (St) and methyl methacrylate (MMA) at 50 °C, but no target polymers were obtained in either case, as shown in Table 1. Although free radicals are generated during the polymerization process, they cannot initiate the polymerization of St and MMA. This indicates that the catalytic polymerization of isoprene in the $Fe(acac)_3/Al^iBu_3$/AIBN system follows a coordination polymerization mechanism. Moreover, the single-crystal structure of the coordination complex formed by AIBN with Fe^{2+} indicates that the azo group offers spatial support for the coordination between the cyano group and Fe^{2+} rather than engaging directly in the coordination.[59] This substantiates that the azo group does not directly participate in coordination at the iron active center, but instead influences the coordination ability of the cyano group with iron *via* electronic effects. In addition, in the AIBN/$Fe(acac)_3/Al^iBu_3$ catalytic system, if the azo groups are completely decomposed, the iron-based catalytic system cannot catalyze the polymerization of IP.

Proposal of Electron Donor with Different Conjugate Groups and Calculation of their Surface ESP Values

Combining the Raman spectroscopy data with the single-crystal literature of AIBN-Fe^{2+} coordination reported in Dalton Transactions[59], the results indicate that the azo group does not participate in coordination with Fe atoms. Instead, they enhance the coordination ability between the cyano groups and Fe through interactions with the cyano groups, thereby improving the catalytic activity of the catalyst system for isoprene polymerization. However, variable-temperature Raman spectra show that the azo group decomposes at elevated temperatures, which could compromise the high-temperature stability of iron-based catalysts and their coordination polymerization activity. According to the experimental results, if it is possible to design and synthesize an electron-donating group that interacts similarly to an azo group, it could ensure both high polymerization activity and stability at high temperatures, thus providing new support for the innovative development of iron-based catalysts. Thus, this work designed conjugated structures, such as benzene rings and vinylene groups, which are structurally similar to the azo group. Dicyano compounds containing benzene rings or vinyl groups were synthesized and selected as electron donors. Isoprene polymerization was conducted under the same conditions to investigate the possibility of replacing the azo group.

As shown in Fig. 5, $Fe(acac)_3$ is a commonly used Fe catalyst in Fe-based catalytic systems. Dicyano compounds with different groups were selected as electron donors and their electrostatic potential (ESP) distributions were calculated at the B3LYP-D3BJ/6-31G (d, p) level. The results reveal that the ESP values on the cyano group surfaces of these compounds are negative, indicating electron-rich regions that facilitate coordination reactions, which is consistent with the results of previous studies.[60] The differences in the ESP values on the cyano group surfaces of the compounds indicate that the conjugated groups regulate the electron cloud density of the cyano N atoms, thereby influencing the coordination

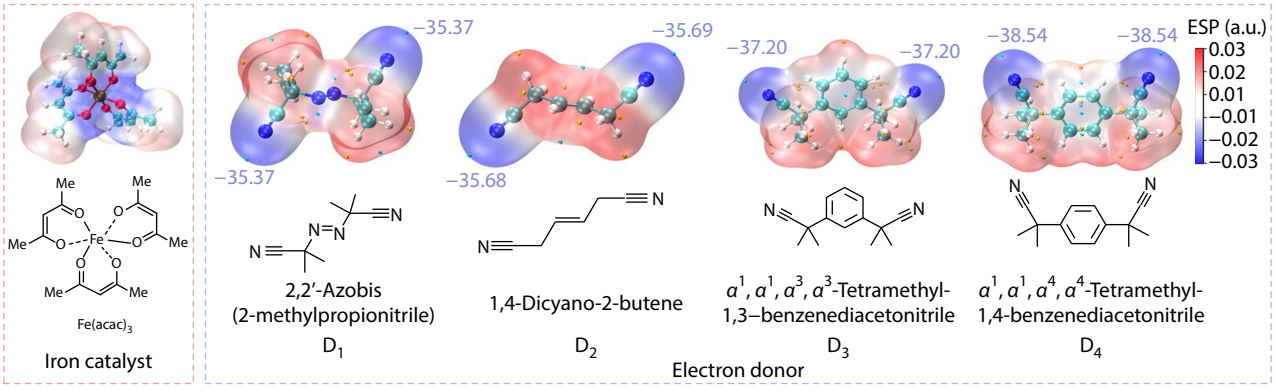

Fig. 5 Molecular structures and ESP analysis of Iron catalyst and four electron donors.

Table 3 Effect of catalyst component under various conditions on the behavior of IP polymerization. [a]

Run	Donor	[IP]/[Fe]	Yield (%)	M_n [b] (×10⁴)	PDI [b]	T_g [c] (°C)	Microstructure [d] (%)		
							3,4	1,2	1,4
1	D_1	2000	99.60	16.0	1.98	−18.9	46.6	5.0	48.4
2		4000	98.75	21.1	1.86	−18.8	47.2	5.1	47.7
3		6000	99.06	26.8	1.76	−18.7	48.5	5.1	46.4
4	D_2	2000	29.62	9.6	2.91	−30.8	42.9	4.9	52.2
5		4000	25.24	10.8	3.54	−31.8	41.8	5.0	53.2
6		6000	8.83	12.0	3.21	−27.9	41.9	5.8	52.3
7	D_3	2000	13.53	3.7	3.13	−26.7	31.2	10.5	58.3
8		4000	2.95	8.7	3.24	−21.5	44.3	7.5	48.2
9		6000	2.34	24.0	1.98	−20.1	46.8	7.5	45.7
10	D_4	2000	2.97	13.0	2.21	−22.0	45.0	7.8	47.2
11		4000	2.41	20.2	1.94	−20.0	47.0	8.0	45.0
12		6000	1.54	22.4	2.53	−20.3	46.8	7.8	45.4

[a] Polymerization conditions: [IP]=1.8 mol·L^{-1}, [Donor]/[Fe]=3, [Al]/[Fe]=20, at 50 °C for 4 h, in hexane; [b] GPC data by trichlorobenzene versus polystyrene standards; [c] Measured using DSC; [d] Determined by NMR.

https://doi.org/10.1007/s10118-026-3581-1

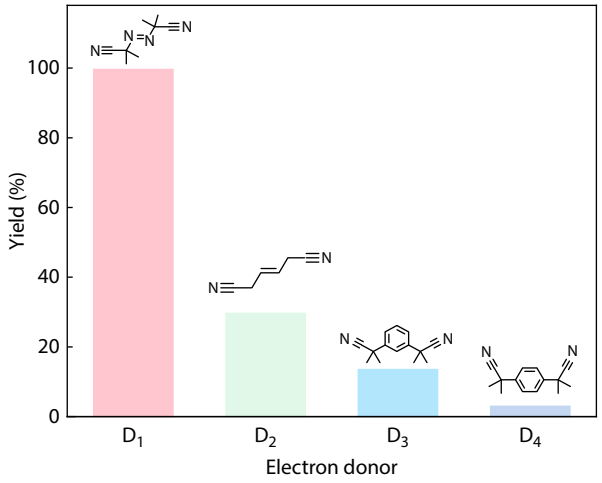

Fig. 6 Effect of electron donor on polymerization behaviors. Polymerization conditions: [IP]=1.8 mol·L^{-1}, [IP]/[Fe]=2000, [Donor]/[Fe]=3, [Al]/[Fe]=20, at 50 °C for 4 h, in hexane.

strength between the cyano groups and iron.[34,40]

Polymerization of Dicyano Compounds Containing Different Conjugated Groups as Electron Donors

Table 3 lists the polymerization activities and polymer microstructures of several electron donors in the ternary system composed of Fe(acac)$_3$/Al^{i}Bu$_3$ catalyzing isoprene polymerization. It can be observed that when dicyano compounds containing azo groups (AIBN, D_1) are used as electron donors, their polymerization activity is significantly higher than that of other dicyano compounds (*e.g.*, aromatic dicyanides and aliphatic dicyanides), with the order of polymerization yield being $D_1 > D_2 > D_3 > D_4$ (Fig. 6). As shown in Fig. 7, the coordination model was simulated using Fe^{2+} as the central metal ion. The model depicts Fe^{2+} coordinated by one acetylacetonate (acac) ligand, one isobutyl (^{i}Bu) group, and three cyano nitrogen atoms (N_{CN}) from electron donors. Specifically, Fe^{2+} forms coordination bonds with the oxygen atoms (O) of acac and nitrogen atoms (N) of the cyano group from AIBN. The isobutyl group was proposed to participate in modulating the spatial configuration around the Fe center. Ultimately, this leads to the formation of a six-coordinate Fe complex with an octahedral geometry. The

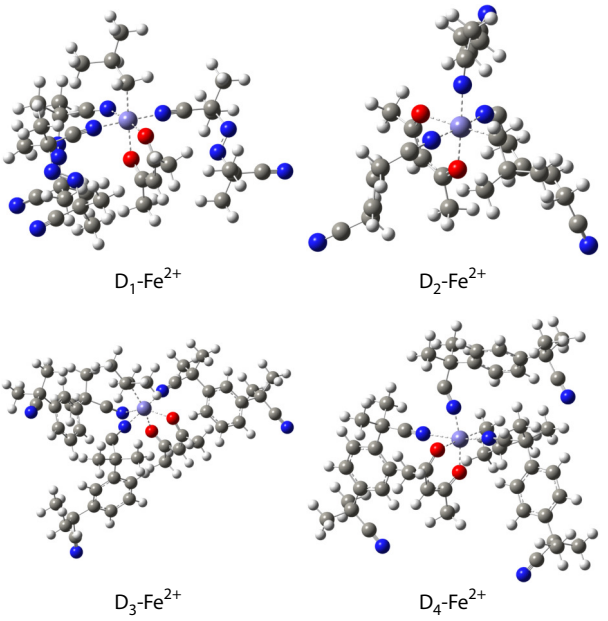

Fig. 7 D_1, D_2, D_3, and D_4 and the coordination model of Fe^{2+}.

Gibbs free energy changes (ΔG) for the coordination reactions between the four electron donors (D_1–D_4) and Fe^{2+} were calculated using density functional theory (DFT) at the B3LYP-D3BJ/6-31G (d, p) level. In this coordination model, only the type of electron-donating ligand coordinated to Fe^{2+} varied, while other conditions remained unchanged. The Gibbs free energy change (ΔG) of the coordination reaction was calculated directly from the Gibbs free energies of all coordination-related species, with units of Hartree (Ha) and electron volts (eV), to reflect the overall thermodynamic trend of the coordination reaction (Table 4). After correction for the enthalpy change ($\Delta H°$) and entropy contribution term ($T\Delta S°$), the thermodynamic Gibbs free energy change ($\Delta G°$) of the coordination reaction under standard conditions (298.15 K, 101.325 kPa) is summarized in Table 5 with units of kilocalories per mole (kcal·mol^{-1}). According to the thermodynamic relationship $\Delta G° = \Delta H° - T\Delta S°$, the negative value of $\Delta G°$ directly reflects the spontaneity of the coordination reaction. The magnitude of $\Delta G°$ allows for a quantitative comparison of ligand-metal coordination abilities: a more

Table 4 Calculation of Gibbs free energy for the coordination reactions of four molecules with Fe^{2+}.

System	3×*G* (Molecule, Ha)	*G* (Fe^{2+}, Ha)	*G* (^{i}Bu, Ha)	*G* (acac, Ha)	*G* (Complex, Ha)	Δ*G* (Ha)	Δ*G* (eV)
D_1–Fe^{2+}	−530.9086	−123.7639	−157.6897	−345.0916	−2219.6259	−0.3549	−9.658
D_2–Fe^{2+}	−341.6531	−123.7639	−157.6897	−345.0916	−1651.8163	−0.3119	−8.487
D_3–Fe^{2+}	−652.4744	−123.7639	−157.6897	−345.0916	−2584.2765	−0.3082	−8.387
D_4–Fe^{2+}	−652.4742	−123.7639	−157.6897	−345.0916	−2584.2716	−0.3037	−8.265

1 Ha = 27.2114 eV = 627.5095 kcal·mol^{-1}; ^{i}Bu = isobutyl; acac = acetylacetone.

Table 5 Calculated thermodynamic data (kcal·mol^{-1}) for coordination reactions between four molecules and Fe^{2+} at 298.15 K and 101.325 kPa.

System	Δ*H*°	*T*Δ*S*°	Δ*G*°
D_1–Fe^{2+}	−286.58	−63.87	−222.71
D_2–Fe^{2+}	−258.37	−62.66	−195.71
D_3–Fe^{2+}	−258.58	−65.17	−193.40
D_4–Fe^{2+}	−256.42	−65.82	−190.60

https://doi.org/10.1007/s10118-026-3581-1

negative $\Delta G°$ value indicates a more stable ligand- Fe^{2+} complex and stronger coordination. Both tables consistently demonstrate that D_1 exhibited the strongest coordination ability with Fe^{2+}, as evidenced by the most negative ΔG value in the thermodynamic data. From the data, coordination ability follows the order $D_1 > D_2 > D_3 > D_4$.[57] This ranking is corroborated by the polymerization activity data, confirming that among the electron donors studied, the azo group was the most effective at enhancing the coordination ability of the cyano group with iron.

CONCLUSIONS

In this study, *in situ* variable-temperature Raman spectroscopy was employed to monitor the coordination behavior of electron donors and their decomposition during polymerization. Molecular simulations were performed to verify our experimental results. The results show that when azo-containing dicyano compounds are used as electron donors, only the cyano group coordinates with the metal center, whereas the azo group does not participate in coordination. However, the azo group constructs a rigid skeleton *via* its non-rotatable double bond to lock the spatial orientation of the cyano group and simultaneously transmits an electron-withdrawing inductive effect through σ-bonds to regulate the electron density and distribution of the nitrogen atom in the cyano group. This effect influences the coordination strength between the cyano group and iron, thereby regulating polymerization activity. *In situ* variable-temperature Raman spectroscopy confirmed that the coordinated azo compounds decomposed at elevated temperatures. However, the polymerization results indicate that the decomposition products cannot initiate the free-radical polymerization of styrene and methyl methacrylate at 50 °C nor can they induce the polymerization of isoprene. These findings verify that AIBN-mediated polymerization follows a coordination polymerization mechanism. Four dicyano compounds with different conjugation groups were prepared. DFT calculations indicated that the degree of influence of the conjugated groups on the coordination ability between the cyano group and the metal center follows the order azo group > carbon-carbon double bond > benzene ring, with the azo group exerting the most significant effect on coordination. The theoretical simulations were consistent with the polymerization results.

In summary, this study explains the origin of the high activity of the AIBN system from both theoretical and practical perspectives. Through molecular simulation of the effect of conjugated moieties in cyano-containing ligands on the cyano coordination behavior, a novel theoretical basis has been established for the rational design of high-efficiency electron donors.

Conflict of Interests

The authors declare no interest conflict.

Electronic Supplementary Information

Electronic supplementary information (ESI) is available free of charge in the online version of this article at http://doi.org/10.1007/s10118-026-3581-1.

Data Availability Statement

Data will be made available from the corresponding author on request.

ACKNOWLEDGMENTS

This work was financially supported by the National Key R&D Program of China (No. 2022YFB3704701), the Natural Science Foundation of Shandong Province (No. ZR2022ME154).

REFERENCES

1 Ayano, S.; Yabe, S. Anionic polymerization of isoprene. I. Polymerization of isoprene by oligomeric dilithium initiator. *Polym. J.* **1970**, *1*, 700–705.
2 Nakayama, Y.; Baba, Y.; Yasuda, H.; Kawakita, K.; Ueyama, N. Stereospecific polymerizations of conjugated dienes by single site iron complexes having chelating n,n,n-donor ligands. *Macromolecules* **2003**, *36*, 7953–7958.
3 Wang, W. X.; Zhao, W. P.; Dong, J.; Zhang, H. Q.; Wang, F.; Liu, H.; Zhang, X. Q. Polyisoprene bearing dual functionalized mini-blocky chain-ends prepared from neodymium-mediated coordinative chain transfer polymerizations. *Chinese J. Polym. Sci.* **2023**, *41*, 720–727.
4 He, Y.; Xu, R.; Zhang, R.; Wang, C. C.; Li, S. Q.; Cao, J.; Tang, M. Z.; Xu, Y. X. Promoted comprehensive properties of polyisoprene rubber with extremely high fatigue resistance enabled by oligopeptide aggregates. *Chinese J. Polym. Sci.* **2023**, *41*, 1250–1260.
5 Rozentsvet, V. A.; Sablina, N. A.; Ulyanova, D. M.; Tolstoy, P. M.; Novakov, I. A. Polymerization of isoprene using cationic catalytic systems based on triethylaluminum. *Dokl. Phys. Chem.* **2021**, *499*, 73–76.
6 Novikova, E. S.; Levkovskaya, E. I.; Senderskaya, E. E.; Chernyavskii, G. G.; Belorukova, T. S. Isoprene polymerization in the presence of phosphate catalytic systems based on a mixture of neodymium and gadolinium salts. *Russ. J. Appl. Chem.* **2023**, *96*, 169–175.
7 Zhou, J.; Zhang, G. G.; Si, C. D.; Jin, M. M.; He, A. H.; Niu, Q. T. Stereoselective synthesis and chain microstructure control of trans-1,4-polyisoprene enabled via $ticl_4$/$mgcl_2$ ziegler-natta catalyst. *Catal. Lett.* **2025**, *155*, 274–274.
8 Bertini, F.; Canetti, M.; Ricci, G. Influence of the composition on crystal phase and thermal behavior of trans-1,4-butadiene/isoprene copolymers. *Macromol. Chem. Phys.* **2007**, *208*, 2551–2559.
9 Wang, B. L.; Cui, D. M.; Lv, K. Highly 3,4-selective living polymerization of isoprene with rare earth metal fluorenyl n-heterocyclic carbene precursors. *Macromolecules* **2008**, *41*, 1983–1988.
10 Gong, D. R.; Dong, W. M.; Hu, J. C.; Zhang, X. Q.; Jiang, L. S. Living polymerization of 1,3-butadiene by a ziegler–natta type catalyst composed of iron(iii) 2-ethylhexanoate, triisobutylaluminum and diethyl phosphite. *Polymer* **2009**, *50*, 2826–2829.
11 Ricci, G.; Leone, G.; Boglia, A.; Boccia, A. C.; Zetta, L. Cis-1,4-alt-3,4 polyisoprene: synthesis and characterization. *Macromolecules* **2009**, *42*, 9263–9267.
12 Liu, B.; Li, L.; Sun, G. P.; Liu, J. Y.; Wang, M. Y.; Li, S. H.; Cui, D. M.

Graphical Abstract

Iron-based Catalysts Catalyzing Isoprene Polymerization: The Effect of Conjugated Groups in Cyanide-containing Electron Donors

Yao Liu, Yao-Guang Liu, Jun-Xin Xu, Qi Yang, Wen-Peng Zhao, Liang Fang, Xiu-Juan Wang, Heng Liu, Chun-Yu Zhang, and Xue-Quan Zhang

Qingdao University of Science & Technology; Suzhou Uropod Precision Instruments Technologies Co., Ltd.

Density functional theory (DFT) calculations reveal that the Δ*G* order of cyano-Fe^{2+} coordination correlates with catalytic polymerization activity, validating Δ*G* as an effective descriptor for electron donor design.

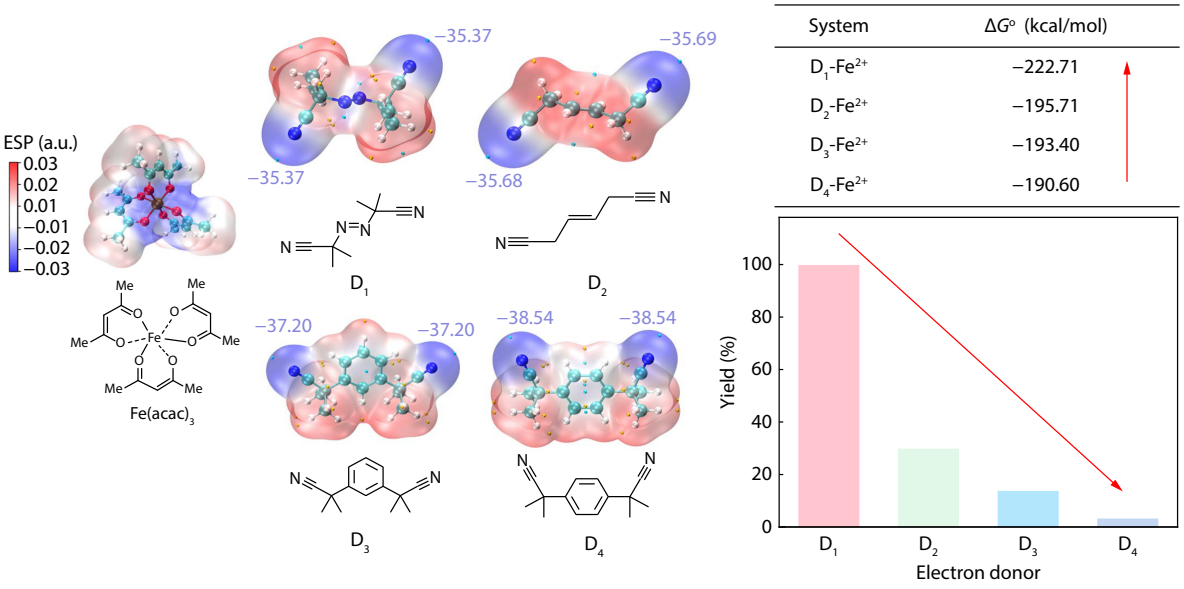

Chinese J. Polym. Sci., 2026 *https://doi.org/10.1007/s10118-026-3581-1*

3,4-polymerization of isoprene by using nsn- and npn-ligated rare earth metal precursors: switching of stereo selectivity and mechanism. *Macromolecules* **2014,** *47*, 4971−4978.

13 Liu, B.; Wang, X. B.; Pan, Y. P.; Lin, F.; Wu, C. J.; Qu, J. P.; Luo, Y.; Cui, D. M. Unprecedented 3,4-isoprene and cis-1,4-butadiene copolymers with controlled sequence distribution by single yttrium cationic species. *Macromolecules* **2014**, *47*, 8524−8530.

14 Liu, B.; Sun, G. P.; Li, S. H.; Liu, D. T.; Cui, D. M. Isoprene polymerization with iminophosphonamide rare-earth-metal alkyl complexes: Influence of metal size on the regio- and stereoselectivity. *Organometallics* **2015**, *34*, 4063−4068.

15 Li, W. X.; Zhao, J. Y.; Zhang, X. Q.; Gong, D. R. Capability of pn^3-type cobalt complexes toward selective (co-)polymerization of myrcene, butadiene, and isoprene: access to biosourced polymers. *Ind. Eng. Chem. Res.* **2019**, *58*, 2792−2800.

16 Gong, D. R.; Tang, F. M.; Xu, Y. C.; Hu, Z. H.; Luo, W. W. Cobalt catalysed controlled copolymerization: an efficient approach to bifunctional polyisoprene with enhanced properties11electronic supplementary information (esi) available. *Polym. Chem.* **2021**, *12*, 1653−1660.

17 Ricci, G.; Leone, G.; Zanchin, G.; Palucci, B.; Boccia, A. C.; Sommazzi, A.; Masi, F.; Zacchini, S.; Guelfi, M.; Pampaloni, G. Highly stereoregular 1,3-butadiene and isoprene polymers through monoalkyl-n-aryl-substituted iminopyridine iron complex-based catalysts: synthesis and characterization. *Macromolecules* **2021**, *54*, 9947−9959.

18 Chen, B. H.; Gong, D. R. Polymerization of butadiene and isoprene using α-diimine cobalt catalysts bearing electron donor at the n-aryl of imine. *J. Organomet. Chem.* **2023**, *994*, 122727.

19 Scoti, M.; De Stefano, F.; Zanchin, G.; Leone, G.; De Rosa, C.; Ricci, G. Synthesis, structure, and properties of poly(isoprene)s of different constitutions and configurations from catalysts based on complexes of nd, co, and fe. *Macromolecules* **2023**, *56*, 4629−4638.

20 Ge, J. J.; Chen, B. H.; Gong, D. R. Catalytic polymerization of isoprene using an ultrahigh active iron(ii) complex with an ortho-modified 1,10-phenanthroline ligand, access to a thermal plastic rubber. *Polym Chem.* **2024**, *15*, 3751−3762.

21 Pan, W.; Chen, H.; Mu, J.; Li, W.; Jiang, F.; Weng, G.; Hu, Y.; Gong, D.; Zhang, X. Synthesis of high crystalline syndiotactic 1,2-polybutadienes and study on their reinforcing effect on cis-1,4 polybutadiene. *Polymer* **2017**, *111*, 20−26.

22 Bazzini, C.; Giarrusso, A.; Porri, L. Diethylbis(2,2′-bipyridine)iron/mao. A very active and stereospecific catalyst for 1,3-diene polymerization. *Macromol. Rapid Commun.* **2002**, *23*, 922−927.

23 Han, Z. Y.; Zhang, Y. Q.; Wang, L.; Zhu, G. Q.; Kuang, J.; Zhu, G. Y.; Xu, G. Q.; Wang, Q. G. 3,4-enhanced polymerization of isoprene catalyzed by side-arm tridentate iminopyridine iron complex with high activity: optimization via response surface methodology. *Polymers* **2023,** *15*, 1231-1244.

24 Zhao, M. M.; Wang, L.; Mahmood, Q.; Jing, C. Y.; Zhu, G. Q.; Zhang, X. H.; Wang, X. W.; Wang, Q. G. Controlled isoprene polymerization mediated by iminopyridine-iron (ii) acetylacetonate pre-catalysts. *Appl. Organomet. Chem.* **2019**, *33*, 4836–4846.

25 Zhao, Y. N.; Xu, S. L.; Yu, Y.; Liu, H.; Wang, F.; Na, L.; Yang, Q.; Zhang, C. Y.; Zhang, X. Q. Preparation and characterization of soft-hard block copolymer of 3,4-ip-b-s-1,2-pbd using a robust iron-based catalyst system. *Polymers* **2024**, *16*, 1172–1186.

26 Xu, S. L.; Zhao, Y. N.; Yu, Y.; Yang, Q.; Na, L. H.; Liu, H.; Zhang, C. Y.; Zhang, X. Q. Study on catalytic behavior of iron-based catalyst with iitp as electron donor in the polymerization of butadiene. *Chinese J. Polym. Sci.* **2024**, *42*, 612–619.

27 Liu, X. J.; Zheng, H.; Wang, X.; Jiang, Z. Y.; Gu, J.; Liu, H.; Zhang, C. Y.; Yang, Q.; Zhang, X. Q. Novel butadiene/isoprene copolymer with predominant 1,2/3,4-units: a tough thermoplastic elastomer material with superior dynamic mechanical properties. *Eur. Polym. J.* **2023**, *196*, 112333–112340.

28 Sun, Y. F.; Zhao, Y. N.; Xu, S. L.; Yu, Y.; Fang, L.; Na, L. H.; Yang, Q.; Wang, F.; Liu, H.; Zhang, C. Y.; Zhang, X. Q. Synthesis and characterization of α-end functionalized 3,4-polyisoprene using fe(acac)$_3$/iitp/al^{i}bu$_3$ catalyst. *Chinese J. Polym. Sci.* **2025**, *43*, 1367–1374.

29 Fischbach, A.; Anwander, R. in *Rare-earth metals and aluminumgetting close in ziegler-type organometallics. Neodymium basedziegler catalysts fundamental chemistry*. Springer Berlin Heidelberg, **2006**, *204*, p. 155–281.

30 Friebe, L.; Nuyken, O.; Obrecht, W., in *Neodymium-basedziegler/natta catalysts and their application in dienepolymerization. Neodymium based ziegler catalysts fundamentalchemistry*. Springer Berlin Heidelberg, **2006**, *204*, p. 1–154.

31 Hu, Z. H.; Xu, Y. C.; Hu, W. H.; Luo, W. W.; Zhao, Y.; Huang, W. Z.; Gong, D. Synthesis and properties of syndiotactic 1,2-polybutadiene catalyzed by iron catalyst with phosphate as additive. *J. Appl. Polym. Sci.* **2020**, *138*, 49686–49694.

32 Liu, X. J.; Yang, Q.; Zhang, C. Y.; Zhang, X. Q.; Liu, H. 3,4-selective polymerization of isoprene by iron-based system: The key role of borate salts for enhancing catalytic activities and broadening 1,10-phenanthroline ligand scope. *Mol. Catal*. **2024,** *559*, 114082-114092.

33 Throckmorton, M. C.; Akron; Ohio. The Goodyear Tire & Rubber Company **1976**, U.S. Pat. 3936432.

34 Swift, H. E.; Bozik, J. E.; Wu, C. Y. Specific catalysis with iron coordination complexes. *J. Catal.* **1970**, *17*, 331–340.

35 Hsu, W. L.; Halasa, A. F. Preparation and characterization of crystalline 3,4-polyisoprene. *Rubber Chem. Technol.* **1994**, *67*, 865–870.

36 Zhang, Z. Y.; Zhang, H. J.; Ma, H. M.; Wu, Y. A novel iron catalyst for the polymerization of butadiene. *J. Mol. Catal.* **1982**, *17*, 65–76.

37 Liu, J. Y.; Li, Y. S.; Liu, J. Y.; Li, Z. S. Ethylene polymerization with a highly active and long-lifetime macrocycle trinuclear 2,6-bis(imino)pyridyliron. *Macromolecules* **2005**, *38*, 2559–2563.

38 Yu, J. G.; Liu, H.; Zhang, W. J.; Hao, X.; Sun, W. H. Access to highly active and thermally stable iron procatalysts using bulky 2-[1-(2,6-dibenzhydryl-4-methylphenylimino)ethyl]-6-[1-(arylimino)ethyl]pyridine ligands. *Chem. Commun.* **2011**, *47*, 3257–3259.

39 Burcher, B.; Breuil, P.-A. R.; Magna, L.; Olivier-Bourbigou, H., in *Iron-catalyzed oligomerization and polymerization reactions*. Iron catalysis II. Springer, Cham, **2015**, p. 217-257.

40 Bi, J. F.; Ge, J. N.; Zhang, X. Q. Study on the polymerization of isoprene catalyzed by Fe(2-EHA)$_3$/Al(i-Bu)$_3$/AIBN. *J. Nat. Sci. Heilongjiang Univ* (in Chinese) **2011,** *28*, 690-695.

41 Na, L. H.; Fan, Y. Q.; Fang, L.; Wang, X. H.; Liu, H.; Zhang, C. Y.; Zhang, X. Q.; Yang, Q. Synergistic n-p coordination enables low-melting, high-crystallinity syndiotactic 1,2-polybutadiene via iron-based catalyst. *Appl. Catal. A* **2025**, *708*, 120594–120601.

42 Saikia, P. J.; Baruah, S. D. Controlled radical polymerization of n-hexadecyl methacrylate mediated by tris(2,2′-bipyridine)iron(iii) complexes. *Polym. Bull.* **2013**, *70*, 3291–3303.

43 Wang, G. X.; Lu, M.; Hou, Z. H.; Gao, Y.; Liu, L. C.; Wu, H. Fe-mediated icar atrp of styrene and acrylonitrile in polyethylene glycol. *J. Appl. Polym. Sci.* **2013**, *131*, 40135–40142.

44 Allan, L. E. N.; MacDonald, J. P.; Nichol, G. S.; Shaver, M. P. Single component iron catalysts for atom transfer and organometallic mediated radical polymerizations: mechanistic studies and reaction scope. *Macromolecules* **2014**, *47*, 1249–1257.

45 Zhang, B. J.; Jiang, X. W.; Zhang, L. F.; Cheng, Z. P.; Zhu, X. L. Fe(iii)-mediated icar atrp in a p-xylene/peg-200 biphasic system: facile and highly efficient separation and recycling of an iron catalyst. *Polym Chem.* **2015**, *6*, 6616–6622.

46 Zhan, X. H. Fe-mediated icar atrp of methyl methacrylate on photoinduced miniemulsion polymerization. *e-Polymers* **2016**, *16*, 41–47.

47 Bower, J. K.; Cypcar, A. D.; Henriquez, B.; Stieber, S. C. E.; Zhang, S. Y. C(sp3)–h fluorination with a copper(ii)/(iii) redox couple. *J. Am. Chem. Soc.* **2020**, *142*, 8514–8521.

48 Chen, X. P.; Qiu, K. Y. 'Living' radical polymerization of styrene with aibn/fecl$_3$/pph$_3$ initiating system via a reverse atom transfer radical polymerization process. *Polym. Int*. **2000,** *49*, 1529-1533.

49 Chen, H. J.; Chen, W. J.; Lin, Y.; Xie, Y.; Liu, S. H.; Yin, J. Visible and near-infrared light activated azo dyes. *Chin. Chem. Lett.* **2021**, *32*, 2359–2368.

50 Mutlaq, D. Z.; Hassan, Q. M. A.; Sultan, H. A.; Emshary, C. A. The optical nonlinear properties of a new synthesized azo-nitrone compound. *Optical Materials* **2021**, *113*, 110815–110828.

51 Frisch, M. J.; Trucks, G. W.; Schlegel, H. B.; Scuseria, G. E.; Robb, M. A.; Cheeseman, J. R.; Scalmani, G.; Barone, V.; Petersson, G. A.; Nakatsuji, H.; Li, X.; Caricato, M.; Marenich, A. V.; Bloino, J.; Janesko, B. G.; Gomperts, R.; Mennucci, B.; Hratchian, H. P.; Ortiz, J. V.; Izmaylov, A. F.; Sonnenberg, J. L.; Williams; Ding, F.; Lipparini, F.; Egidi, F.; Goings, J.; Peng, B.; Petrone, A.; Henderson, T.; Ranasinghe, D.; Zakrzewski, V. G.; Gao, J.; Rega, N.; Zheng, G.; Liang, W.; Hada, M.; Ehara, M.; Toyota, K.; Fukuda, R.; Hasegawa, J.; Ishida, M.; Nakajima, T.; Honda, Y.; Kitao, O.; Nakai, H.; Vreven, T.; Throssell, K.; Montgomery Jr., J. A.; Peralta, J. E.; Ogliaro, F.; Bearpark, M. J.; Heyd, J. J.; Brothers, E. N.; Kudin, K. N.; Staroverov, V. N.; Keith, T. A.; Kobayashi, R.; Normand, J.; Raghavachari, K.; Rendell, A. P.; Burant, J. C.; Iyengar, S. S.; Tomasi, J.; Cossi, M.; Millam, J. M.; Klene, M.; Adamo, C.; Cammi, R.; Ochterski, J. W.; Martin, R. L.; Morokuma, K.; Farkas, O.; Foresman, J. B.; Fox, D. J. *Gaussian 16 rev. C.01*, Wallingford, CT, **2016**.

52 Lu, T.; Chen, F. Multiwfn: A multifunctional wavefunction analyzer. *J. Comput. Chem.* **2012**, *33*, 580–592.

53 Humphrey, W.; Dalke, A.; Schulten, K. Vmd: Visual molecular dynamics. *J. Mol. Graph.* **1996**, *14*, 33–38.

54 Kuznetsov, M. L.; Bokach, N. A.; Kukushkin, V. Y.; Pakkanen, T.; Wagner, G.; Pombeiro, A. J. L. Metal-assisted coupling of oximes and nitriles: a synthetic, structural and theoretical study. *J. Chem. Soc., Dalton Trans*. **2000,** 4683-4693.

55 Kuznetsov, M. L.; Kukushkin, V. Y.; Haukka, M.; Pombeiro, A. J. L. 1,3-dipolar cycloaddition of nitrile oxides to free and pt-bound nitriles: a theoretical study of the activation effect, reactivity and

mechanism. *Inorg. Chim. Acta* **2003,** *356*, 85-94.
56 Kuznetsov, M. L.; Bokach, N. A.; Kukushkin, V. Y.; Dement'ev, A. I. Theoretical study of ammonia nucleophilic addition to nitriles in platinum complexes. *Russ. J. Gen. Chem.* **2009**, *79*, 232−241.
57 Casella, G.; Guerra, C. F.; Carlotto, S.; Sgarbossa, P.; Bertani, R.; Casarin, M. New light on an old debate: Does the rcn-ptcl2 bond include any back-donation Rcn←ptcl2 backbonding vs. The ir vcn blue-shift dichotomy in organonitriles-platinum(ii) complexes. A thorough density functional theory — energy decomposition analysis study. *Dalton Trans.* **2019**, *48*, 12974−12985.
58 Knobelsdorf, J. A.; Shepherd, T. A.; Tromiczak, E. G.; Zarrinmayeh, H.; Zimmerman, D. M.; Indianapolis, In. Eli Lilly and Company **2001**, PCT Pat. WO 01/96289 A1.
59 Chainok, K.; Neville, S. M.; Moubaraki, B.; Batten, S. R.; Murray, K. S.; Forsyth, C. M.; Cashion, J. D.; Haller, K. J. Synthesis, structures and spin crossover properties of infinite 3d frameworks of iron(ii) containing organodinitrile bridging ligands. *Dalton Trans.* **2010**, *39*, 10900−10909.
60 Macchi, P.; Ragaini, F.; Casati, N.; Krawczuk, A.; Sironi, A. Experimental and theoretical electron density of intermediates in palladium-phenanthroline catalyzed carbonylation of amines and reductive carbonylation of nitroarenes. *J. Comput. Chem.* **2018**, *39*, 581−586.

https://doi.org/10.1007/s10118-026-3581-1